



*Citation for published version:*

Djabri, A, Guy, RH & Delgado-Charro, MB 2012, 'Passive and iontophoretic transdermal delivery of phenobarbital: implications in paediatric therapy', *International Journal of Pharmaceutics*, vol. 435, no. 1, pp. 76-82. <https://doi.org/10.1016/j.ijpharm.2012.02.026>

*DOI:*

[10.1016/j.ijpharm.2012.02.026](https://doi.org/10.1016/j.ijpharm.2012.02.026)

*Publication date:*

2012

*Document Version*

Peer reviewed version

[Link to publication](#)

NOTICE: this is the author's version of a work that was accepted for publication in *International Journal of Pharmaceutics*. Changes resulting from the publishing process, such as peer review, editing, corrections, structural formatting, and other quality control mechanisms may not be reflected in this document. Changes may have been made to this work since it was submitted for publication. A definitive version was subsequently published in *International Journal of Pharmaceutics*, vol 435, issue 1, 2012, DOI 10.1016/j.ijpharm.2012.02.026

## University of Bath

### General rights

Copyright and moral rights for the publications made accessible in the public portal are retained by the authors and/or other copyright owners and it is a condition of accessing publications that users recognise and abide by the legal requirements associated with these rights.

### Take down policy

If you believe that this document breaches copyright please contact us providing details, and we will remove access to the work immediately and investigate your claim.

1  
2  
3  
4  
5  
6  
7  
8  
9  
10  
11  
12  
13  
14  
15  
16  
17  
18  
19  
20  
21  
22  
23  
24

**Passive and iontophoretic transdermal delivery of phenobarbital:  
implications in paediatric therapy.**

<sup>1,2</sup>Asma Djabri, <sup>1</sup>Richard H. Guy and <sup>1,3</sup> M. Begoña Delgado-Charro

<sup>1</sup> Department of Pharmacy & Pharmacology, University of Bath, Claverton  
Down, BA2 7AY, UK

<sup>2</sup> Present address: Asma Djabri: ITH Pharma, Unit 4 Premier Park, Premier Park  
Road, London, NW10 7NZ, UK

E- mail addresses:

Asma Djabri: asma.djabri@ithpharma.com

Richard H. Guy : R.H.Guy@bath.ac.uk

M. Begoña Delgado-Charro: B.Delgado-Charro@bath.ac.uk

<sup>3</sup> Corresponding author:

Department of Pharmacy & Pharmacology, University of Bath, Claverton Down,  
BA2 7AY, UK

Phone: +44 (0) 1225 383969

Fax: +44 (0) 1225 386114

B.Delgado-Charro@bath.ac.uk

25           **Abstract**

26           The objective of this investigation was to evaluate phenobarbital transdermal  
27 delivery for possible use in paediatric care. *In vitro* experiments were performed  
28 using intact pig skin and barriers from which the stratum corneum had been stripped  
29 to different extents to model the less resistant skin of premature babies. Cathodal  
30 iontophoretic delivery of phenobarbital was superior to anodal transport and  
31 optimised delivery conditions were achieved by reduction of competing co-ion  
32 presence in the drug formulation. Phenobarbital transport across intact or partially  
33 compromised skin was controlled by iontophoresis which was more efficient than  
34 passive diffusion. Across highly compromised skin, however, passive diffusion  
35 increased drastically and iontophoretic control was lost. Overall, this study  
36 demonstrates the feasibility of phenobarbital transdermal delivery for paediatric  
37 patients.

38

39           **Key words:** paediatric, transdermal, iontophoresis, phenobarbital, premature,  
40 tape-stripping

41

## 42           **1. Introduction**

43           Phenobarbital is a barbiturate drug used in the treatment of different forms of  
44   paediatric epilepsy and status epilepticus (BNF for children, 2011) being the first-line  
45   choice to control neonatal seizures (Lehr, 2005, Blume, 2009, Ouvrier, 1982). It is  
46   also used to treat neonatal abstinence syndrome both in the case of sedative-  
47   hypnotic withdrawal and as an adjunct therapy to treat opiate withdrawal symptoms  
48   (Bio, 2011, Finnegan, 2005, Osborn, 2010). Due to developmental changes in  
49   children, the pharmacokinetics of phenobarbital are highly variable in this  
50   population; doses are, therefore, titrated according to the individual's response for  
51   adequate seizure control while avoiding, at the same time, adverse effects due to  
52   supra-optimal levels (BNF for children 2011, Finnegan, 2005, Heimann, 1977, Lehr,  
53   2005, Touw, 2000). The target therapeutic plasma concentrations are set between  
54   40 and 180  $\mu\text{mol}\cdot\text{mL}^{-1}$  depending on the application envisaged (Bio, 2011, Finnegan,  
55   2005, Lehr, 2005, Touw, 2000). Heimann (1977) found that the elimination half-life  
56   of phenobarbital in mature neonates ( $118 \pm 16$  h) is significantly longer than that in  
57   infants of 2-12 months ( $63 \pm 5$ h) and in children aged 2-5 years ( $68 \pm 3$ h). Touw  
58   (2000) found that the elimination half-life varied between 48 and 147 h for a group  
59   of 19 term and preterm neonates. Phenobarbital clearance is slowest for newborns,  
60   increasing rapidly during the first two weeks of life and reaching a peak at 6-12  
61   months. On the other hand, the total clearance normalized per kg body weight  
62   appears to decrease with increasing maturity (Touw, 2000, Lehr 2005). The average  
63   clearance of phenobarbital in neonates is about  $4.3 \text{ mL}\cdot\text{h}^{-1}\cdot\text{kg}^{-1}$  (Touw, 2000)  
64   whereas, for older children, a mean value of approximately  $8 \text{ mL}\cdot\text{h}^{-1}\cdot\text{kg}^{-1}$  is observed

65 (Botha, 1995, Heimann, 1977, Winter, 2010). Phenobarbital distribution volume  
66 decreases with age and with gestational age; Touw (2000) reported a mean volume  
67 of distribution of  $0.71 \pm 0.21 \text{ L.kg}^{-1}$  for term and preterm neonates. Heimann (1977)  
68 used a two-compartmental model to describe phenobarbital kinetics in children of  
69 several age groups, from term neonates up to 5 years old, and found a modest age  
70 dependency for both the volume of distribution in the steady-state and the volume  
71 of the central compartment; the values reported for  $V_{ss}$  ranged from  $0.85 \pm 0.06$  to  
72  $0.67 \pm 0.07 \text{ L.kg}^{-1}$ .

73 Phenobarbital is well absorbed orally (Winter, 2010); however, tablets are not  
74 suitable for neonates and young children and the only approved oral alternative  
75 described in the BNF (BNF for children, 2011) contains 38% ethanol. Regular  
76 administration of this elixir may cause alcohol toxicity, especially in neonates. As  
77 consequence, extemporaneous formulations, including suspensions from crushed  
78 tablets, are sometimes prepared (Cober, 2007, Colquhoun-Flannery 1992). Slow  
79 intravenous injections are also frequently used, but care must be taken to dilute the  
80 parenteral formulation ( $200 \text{ mg.mL}^{-1}$  phenobarbital in 90% propylene glycol) to  
81 provide suitable doses for young infants and children and to avoid accumulation of  
82 the cosolvent (Allagaert, 2010, BNF for children 2011).

83 Passive transdermal delivery of phenobarbital has been suggested as an  
84 alternative route of administration (Bonina, 1993). In this earlier *in vitro* study, drug  
85 flux across excised skin from premature infants (29 – 35 weeks gestational age) was  
86 approximately 4-fold greater ( $0.4 \pm 0.13 \text{ }\mu\text{g.h}^{-1}.\text{cm}^{-2}$ ) than that ( $0.1 \pm 0.02 \text{ }\mu\text{g.h}^{-1}.\text{cm}^{-2}$ )  
87 through either adult or full-term (37 – 40 weeks gestational age) skin. In general,  
88 fluxes were inversely related to the gestational age of the donor. It was estimated

89 that a 25 cm<sup>2</sup> transdermal patch would be sufficient to provide an average steady-  
90 state plasma concentration of 3.2 mg.L<sup>-1</sup> (14 μM) for a 1 kg neonate. However, the  
91 feasibility of the approach employed may be questioned as the vehicle used in this  
92 work was pure ethanol which is known to be toxic to preterm newborns when  
93 absorbed across the skin from cleaning products (Harpin, 1982). Further, the total  
94 skin surface area of a neonate varies between 0.03 and 0.25 m<sup>2</sup> depending on  
95 gestational age (Touw, 2000). While there are no guidelines concerning the  
96 maximum acceptable size of a transdermal patch for neonatal use, values in the  
97 range of 1-10 cm<sup>2</sup> would be consistent with current usage in adults: for these  
98 individuals, total skin area is ~ 2 m<sup>2</sup>, while largest patches in use are in the order of  
99 50 cm<sup>2</sup>. Finally, the systemic concentration achievable (14 μM) is lower than the  
100 recommended target for paediatric patients (40 – 180 μM).

101 Here, an optimised approach to the delivery of phenobarbital across both intact  
102 and premature skin is proposed. Using iontophoresis as a physical enhancement  
103 method, improved delivery rates of the drug are achieved compared to passive  
104 diffusion suggesting that smaller patch sizes can be used to attain therapeutic  
105 systemic levels. With iontophoresis, the much more water-soluble sodium salt of  
106 phenobarbital is preferred eliminating the need for incorporation of co-solvents  
107 (such as ethanol) in the topical formulation. The aqueous solubility of sodium  
108 phenobarbital (molecular weight = 254.2 Da) is 1 g/mL, approximately 1000-fold  
109 greater than that of the free acid. Intact and premature neonatal skin barriers were  
110 modelled *in vitro* using pig skin, from which stratum-corneum was differentially tape-  
111 stripped as previously described (Sekkat, 2004a, 2004b).

112

113

114

## 115 **2. Materials and methods**

### 116 **2.1 Chemicals**

117 Sodium phenobarbital (PHEN), silver wire (99.99%), silver chloride (99.999%),  
118 sodium hydroxide pellets, and NaOH 50% solution (ion chromatography eluent  
119 grade) were purchased from Sigma Aldrich (Gillingham, UK). Potassium dihydrogen  
120 phosphate, HEPES (4-(2-hydroxyethyl)-1-piperazine ethanesulfonic acid (HEPES) and  
121 sodium chloride were obtained from Acros (Geel, Belgium). Acetonitrile and  
122 hydrochloric acid were provided by Fisher Scientific (Loughborough, UK). All reagents  
123 were at least analytical grade and deionised water (resistivity  $\geq 18.2 \text{ M}\Omega\cdot\text{cm}$ ,  
124 Barnsted Nanopure Diamond™, Dubuque, IA) was used for the preparation of all  
125 solutions.

### 126 **2.2 Skin**

127 Fresh pig skin was obtained from a local slaughterhouse, cleaned under cold  
128 running water, and stored in a refrigerator until the following day. Abdominal skin  
129 was dermatomed (Zimmer™ Electric Dermatome, Dover, Ohio) to a nominal  
130 thickness of 750  $\mu\text{m}$ , cut into (10 x 10  $\text{cm}^2$ ) pieces, wrapped individually in Parafilm™,  
131 and then kept in a freezer (-20 °C) until use. Prior to the experiments, the skin was  
132 thawed at room temperature for 30 minutes and excess hair was cut with scissors.  
133 The large piece of skin was then cut into 4 portions. One served as representative of  
134 the intact skin barriers while the others were subjected a tape-stripping procedure  
135 to create different degrees of compromised skin. The intact barriers were  
136 characterized by transepidermal water loss (TEWL) measurements (AquaFlux AF-102,

137 Biox Systems Ltd., London, UK) of  $9.0 \pm 1.7 \text{ g}\cdot\text{m}^{-2}\cdot\text{h}^{-1}$ . The three other pieces of skin  
138 were repeatedly tape-stripped (2 x 2 cm, Scotch Book Tape, 3M, St. Paul, MN) to  
139 progressively remove the stratum corneum. A 1.5 x 1.5 cm<sup>2</sup> template was affixed  
140 onto the skin before the stripping procedure started to ensure the removal of  
141 stratum corneum was from the same location. Periodic measurement of TEWL  
142 allowed the degree of barrier compromise to be quantified and full barrier  
143 impairment was defined when the removal of three consecutive tape strips did not  
144 alter TEWL. The number of tape strips required to produce a fully compromised  
145 barrier varied between 13 and 23. The second and third pieces of skin were tape-  
146 stripped until TEWL reached values of between 20-40% and 60-80%, respectively, of  
147 the TEWL recorded for the fully compromised barrier. Thus, three levels of barrier  
148 function impairment were studied: 20-40% (Intermediate “less” barrier), 60-80%  
149 (Intermediate “plus” barrier), and 100% (fully compromised barrier).

### 150 **2.3 Iontophoresis set-up**

151 Side-by-side two-compartment diffusion cells (active transport area = 0.78 cm<sup>2</sup>,  
152 volume = 3.3 mL) were used in all experiments. The skin was mounted between the  
153 two chambers with the epidermal side oriented towards the cathode compartment.  
154 The receptor chamber always held 154 mM sodium chloride solution (unbuffered,  
155 pH ~ 6). Prior to the start of the transport study, the skin was left for 30 minutes in  
156 contact with the donor vehicle without drug, and 154 mM sodium chloride in the  
157 receptor chamber. The compartments were then emptied and refilled with a donor  
158 solution containing sodium phenobarbital and with fresh receptor solution. Both  
159 compartments were magnetically stirred (Multipoint-6 stirrer, Thermo Scientific  
160 Variomag, Cole-Parmer, UK) throughout the experiment. A direct constant current of



161 0.4 mA ( $0.5 \text{ mA}\cdot\text{cm}^{-2}$ ) was delivered using Ag/AgCl electrodes and a power supply  
162 (KEPCO 1000M, Flushing, NY, USA). Hourly samples (0.5 mL) of the receptor phase  
163 were withdrawn for analysis and replaced with fresh receptor solution. Experiments,  
164 which compared phenobarbital iontophoretic delivery through different skin  
165 barriers, also monitored passive permeation (same donor solution) post-current  
166 termination. Separate passive diffusion controls (no current) through both intact and  
167 compromised skin were also performed. The details of the experiments performed  
168 are in Table 1.

169 Another series of experiments examined the effect of iontophoresis on the  
170 passive permeability of intact skin to phenobarbital. Prior to the permeation study,  
171 and in the absence of phenobarbital (i.e., with a donor compartment containing  
172 water, pH 8.5, and receptor compartment containing unbuffered 154 mM NaCl), a  
173 0.4 mA current was applied for 5 hours. At this point, the current was terminated  
174 and the compartments were then emptied and refilled with a donor solution  
175 containing phenobarbital and with fresh receptor solution. Passive diffusion was  
176 then followed for 24 hours. To account for any effect of skin hydration during the  
177 pre-iontophoresis, the same experiment was repeated without application of current  
178 and with the donor and receptor compartments being filled with water and 154 mM  
179 NaCl, respectively.

#### 180 **2.4 Phenobarbital and chloride analysis**

181 Quantification of phenobarbital was performed by high performance liquid  
182 chromatography with UV detection (215 nm). The method was modified from a  
183 previous publication (Sekkat, 2004b) and used a Jasco HPLC system (PU-980 pump  
184 with an AS-1595 autosampler, a UV-975 UV-VIS detector, and an Acclaim 120, C18

185 (150 x 4.6 mm, 5 $\mu$ m) reversed-phase column (Dionex, UK) which was thermostated  
186 at 30 °C). The mobile phase, pumped at 1 mL.min<sup>-1</sup>, consisted of phosphate buffer  
187 (0.067 M KH<sub>2</sub>PO<sub>4</sub>) and acetonitrile (70:30) and the pH was adjusted to 6 with NaOH.

188 Chloride was analysed by ion chromatography with suppressed conductivity  
189 detection (Sylvestre, 2008) using a Dionex system (Sunnyvale, CA) comprising a GP-  
190 50 gradient pump, an AS-50 autosampler and thermal compartment, and an ED-50  
191 electrochemical detector. The mobile phase, 35 mM NaOH, was pumped isocratically  
192 (1 mL.min<sup>-1</sup> flow rate) through a Dionex IonPac™ AS16 (250 x 4 mm) column  
193 thermostated at 30°C and connected to a Dionex ASRS Ultra II suppressor (4 mm) set  
194 at a current of 90 mA.

## 195 **2.5 Data analysis and statistics**

196 Data analysis was performed using Graph Pad Prism V.5.00 (Graph Pad Software  
197 Inc., CA, USA). Unless otherwise stated, data are presented as the mean  $\pm$  standard  
198 deviation. Transport fluxes were calculated as the amounts delivered during a  
199 permeation period divided by the length of that period. Statistical significance was  
200 set at  $p < 0.05$ . Comparisons made between different sets of data were assessed by  
201 either a two-tailed unpaired t-test (for 2 groups) or a one-way ANOVA (for > 2  
202 groups) followed by Tukey's post-test. Comparison of fluxes at different times was  
203 assessed by repeated-measures ANOVA followed by Tukey's post-test.

204 The corrected transference number ( $t_{COR,PHEN}$ ) of phenobarbital was computed  
205 according to Faraday's law (Phipps, 1992):

$$206 \quad t_{PHEN} = \frac{J_{COR,PHEN} \cdot z \cdot F}{I} \quad \text{Equation 1}$$

207 where,  $J_{COR,PHEN}$  is the corrected flux,  $I$  is the current intensity applied,  $F$  is faraday's  
208 constant, and  $z$  the absolute value of the drug valence. Transference numbers were  
209 calculated from the corrected fluxes representing those observed after 5 hours  
210 iontophoresis ( $J_{PHEN}$ ) minus the passive diffusion rate 5 hours post-current  
211 termination.

### 212 **3. Results and discussion**

#### 213 **3.1 Passive diffusion across intact skin**

214 The passive diffusion of phenobarbital from a 50 mM aqueous drug solution (pH  
215 8.5) across (i) untreated skin, (ii) skin pre-treated with 0.4 mA current for 5 hours,  
216 and (iii) skin hydrated for 5 hours is shown in Figure 1 in terms of drug permeation as  
217 a function of time. The cumulative amounts transported ( $\pm$  SD) 24 hours post-drug  
218 application were:  $91.7 \pm 33.7$ ,  $415 \pm 125$ , and  $222 \pm 35.5$  nmol.cm<sup>-2</sup> for untreated,  
219 pre-iontophoresed, and pre-hydrated skin, respectively. Passive diffusion across pre-  
220 iontophoresed skin was significantly higher than through untreated ( $p < 0.01$ ) and  
221 pre-hydrated ( $p < 0.05$ ) skin. Increased permeability of skin previously exposed to  
222 direct current has been previously reported (Green, 1992).

#### 223 **3.2 Iontophoretic delivery across intact skin**

224 The first donor solution tested was 50 mM sodium phenobarbital in water (pH  
225 8.5) where the drug ( $pK_a = 7.3$ ) (Merk Index, 2006) was ~93 % ionised. Cathodal  
226 iontophoresis resulted in drug delivery that was 385-fold higher than passive  
227 diffusion (Figure 2). After only 1 hour of current application, the phenobarbital flux  
228 was  $222 \pm 94.4$  nmol.h<sup>-1</sup> increasing to  $387 \pm 57.2$  nmol.h<sup>-1</sup> by 3 hours. At the end of  
229 the experiment (5 h), the flux was  $341 \pm 64.5$  nmol.h<sup>-1</sup>.

230 A second series of iontophoresis experiments compared anodal *versus* cathodal  
231 delivery of phenobarbital at pH 7.4 where phenobarbital exists in essentially equal  
232 concentrations of the ionized and unionized forms. The former, of course, can be  
233 delivered from the cathode by electro-repulsion, while the latter may be transported  
234 from the anode by electro-osmosis. A donor concentration of 15 mM was used  
235 because of phenobarbital's lower solubility at this pH. Chloride ions are required to  
236 ensure adequate electrochemistry at the anode, and 50 mM NaCl was therefore  
237 added to both the cathodal and anodal solutions. Cathodal iontophoresis (Figure 3)  
238 was much more efficient than anodal. When the contribution of passive diffusion  
239 was taken into account, the corrected cathodal and anodal fluxes at 5 hours were  
240  $42.4 \pm 13.3$  and  $7.1 \pm 3.8$  nmol.h<sup>-1</sup>, respectively. These results are in good agreement  
241 with previous data (e.g., for 5-fluorouracil (Merino, 1999) and for phenytoin  
242 (Leboulanger,2004)) which showed that electromigration is a much more efficient  
243 transport mechanism than electroosmosis. The reduced cathodal delivery observed  
244 here relative to that observed at pH 8.5 is explained by the lower concentration of  
245 ionized drug employed, decreasing from 46.3 mM (~93 % of 50 mM) to 7.5 mM  
246 (~50% of 15 mM) and by the presence of 50 mM competing chloride ions in the pH  
247 7.4 experiment.

248 The effect of co-ion competition on cathodal delivery by electro-repulsion was  
249 then investigated. In an initial experiment, a 15 mM PHEN solution, the pH of which  
250 had been adjusted to 7.4 with HCl was used, resulting in introduction of Cl<sup>-</sup> at a  
251 concentration of approximately 6 mM. As this represents a lower level of chloride  
252 ions compared to the earlier experiment, an increase in  $t_{\text{PHEN}}$  and PHEN flux might  
253 have been expected. However, the concentration of competing chloride increases

254 above the initial 6 mM during the experiment because of the gradual release of Cl<sup>-</sup>  
255 from the cathode as the electrochemistry reduces AgCl to Ag (Figure 4). This implies  
256 that transport number of the drug would decrease as the experiment proceeds.

257 A subsequent experiment attempted to mitigate the impact of chloride  
258 accumulation on the cathodal flux of PHEN by refreshing the donor solution every  
259 hour. In a related experiment, 10 mM HEPES was employed as a buffer for the 15  
260 mM sodium phenobarbital donor solution. This provided good buffer capacity  
261 without requiring any adjustment to pH 7.4 with HCl (thereby avoiding the  
262 introduction of extra chloride ions). Again, to counter the build-up of chloride ions  
263 released from the electrode, the donor solution was refreshed hourly. It was  
264 calculated that Cl<sup>-</sup> release from the cathode would contribute (in the diffusion cells  
265 used) a concentration of 4.5 mM for every hour of 0.4 mA current applied. Figure 4  
266 illustrates the anticipated evolution of chloride concentration in the donor solution  
267 as a function of time under the experimental conditions employed. The predicted  
268 values agree closely with those measured experimentally by ion chromatography.

269 The PHEN fluxes were inversely related to the Cl<sup>-</sup> concentration present in the  
270 donor solution after 5 hours of current application. The greater the co-ion  
271 competition with PHEN, the lower the drug transport (Figure 4). Chloride  
272 accumulation in the cathodal chamber plays a key role in the iontophoretic delivery  
273 of negatively-charged drugs as previously demonstrated for dexamethasone  
274 phosphate (Sylvestre, J.P., 2008a. 2008b) and needs careful optimization.

275 The transport number of phenobarbital ( $t_{\text{PHEN}}$ ) was linearly proportional ( $r^2 \approx$   
276 0.80) to the drug's molar fraction in the vehicle (Figure 5). Following the principles  
277 demonstrated by Mudry et al. (2006) for cation electrotransport, and assuming their

278 validity for the anionic PHEN, the maximum transport number of the drug at pH 7.4,  
279 i.e., in the absence of competing co-ions, is estimated to be 0.035 (determined by  
280 substitution of  $X_{\text{PHEN}}=1$  in the linear regression equation given in Figure 5).

### 281 **3.3 Permeation across compromised skin**

282 The objective of this part of study was to examine the permeation of  
283 phenobarbital across barriers representative of those found in premature neonates  
284 whose stratum corneum may be absent or not fully developed. Three impaired levels  
285 of barrier function were evaluated against intact skin for passive as well as  
286 iontophoretic delivery of the drug. The average TEWL measurements ( $\text{g}\cdot\text{m}^{-2}\cdot\text{h}^{-1}$ )  
287 across the different skin barriers were as follows:  $11 \pm 1$ ,  $44 \pm 10$ ,  $114 \pm 20$ , and  $158 \pm$   
288  $25$ , respectively, for intact, intermediate “less” (20 – 40 %), intermediate “plus” (60 –  
289 80 %), and fully compromised skin. The TEWL values were significantly higher than  
290 those reported in previous studies, which validated the usefulness of serially  
291 stripped pig skin as a model for that of the developing neonate and subsequently  
292 employed the approach to predict the transdermal permeation of phenobarbital,  
293 caffeine, and lidocaine (Sekkat 2004a, 2004b). The discrepancy is between a factor of  
294 two and four and is probably due to the different TEWL devices employed in the two  
295 studies (i.e., the study closed-chamber evaporimeter (AquaFlux AF102, Biox) used  
296 here versus an open-chamber instrument (EP1, Servomed) used before (Farahmand,  
297 2009, Imhof 2009). Other factors may have played a part, such as the number of  
298 tape-strips used to remove the stratum corneum, and the pressure with which the  
299 tapes were applied (Escobar-Chavez, 2008, Rubio et al., 2011).

300 Passive diffusion of phenobarbital increased dramatically as the stratum  
301 corneum was progressively compromised (Figure 6). The flux at 5 hours through

302 intact skin was only  $0.9 \pm 0.2 \text{ nmol.h}^{-1}$ , but increased to  $810 \pm 251 \text{ nmol.h}^{-1}$  for fully  
303 compromised skin. Transport through barriers with intermediate levels of  
304 impairment levels fell between these two extremes:  $31 \pm 12 \text{ nmol.h}^{-1}$  and  $561 \pm 179$   
305  $\text{nmol.h}^{-1}$  for 20-40 % and 60-80 % of barrier disruption, respectively.

306 Previously, a similar phenobarbital permeation rate across intact full-thickness  
307 pig ear skin was measured when the drug was delivered from a saturated solution of  
308 the unionised drug (4.3 mM) at pH 5 (Sekkat, 2004b). Permeation across fully  
309 compromised skin was ~30 times higher than that through the intact barrier. In  
310 contrast, the enhancement factor observed in this work was more than 900-fold due,  
311 at least in part, to the fact that most of the drug was ionised (~3.7 mM unionized)  
312 and hence in a less favourable form for passive permeation. With progressive  
313 removal of the stratum corneum, the ionised and neutral forms of phenobarbital  
314 permeated through the less-resistant skin barrier at much higher rates. Similar  
315 behaviour has been seen for 5-fluorouracil (Fang, 2004), with removal of the stratum  
316 corneum leading to an increase in passive diffusion from  $< 0.03 \mu\text{mol.cm}^{-2}$  in 6 hours  
317 to approximately  $17 \mu\text{mol.cm}^{-2}$  a difference of more than 550-fold.

318 Figure 6 summarizes the iontophoretic delivery of phenobarbital through  
319 compromised skin barriers. The fluxes measured during 5 hours of iontophoresis (0.4  
320 mA) application followed by 5 hours of passive diffusion are shown. Table 2 presents  
321 the fluxes during the last hour of the permeation studies. The iontophoretic fluxes  
322 observed increased with the level of skin impairment but complete removal of the  
323 stratum corneum only resulted in a 3.6-fold enhancement relative to intact skin  
324 (Table 2). When the contribution of passive diffusion is taken into account, the  
325 corrected iontophoretic fluxes, and the corresponding  $t_{\text{PHEN}}$ , are very similar for all

326 skin barriers tested (Table 2). In fact, no significant differences were found between  
327 these values. It follows that while iontophoretic flux remained constant and  
328 independent of the skin barrier function, passive diffusion increased remarkably as  
329 the skin was progressively compromised and eventually overshadowed any benefits  
330 from iontophoresis. Qualitatively, these results are consistent with those reported  
331 for lidocaine hydrochloride (Sekkat, 2004b), for which the total iontophoretic  
332 delivery was practically the same across intact ( $1.8 \pm 0.5 \text{ mg.cm}^{-2}$ ) and tape-stripped  
333 skin ( $1.9 \pm 0.3 \text{ mg.cm}^{-2}$ ). In contrast, the passive permeability of lidocaine HCL  
334 increased from  $7 \times 10^{-4} \pm 4 \times 10^{-4} \text{ mg.cm}^{-2}$  across intact skin to  $0.1 \pm 0.07 \text{ mg.cm}^{-2}$   
335 through a fully tape-stripped barrier. Quantitatively, however, the difference  
336 between the behaviour of lidocaine and phenobarbital is important. In the case of  
337 lidocaine, the passive diffusion of the drug even across fully-compromised skin is still  
338 an order of magnitude smaller than iontophoretic delivery; electrotransport can be  
339 used, therefore, to control drug input independent of the status of skin barrier  
340 function. For phenobarbital, on the other hand, passive transport increases  
341 significantly with progressive derangement of the barrier, ultimately overwhelming  
342 iontophoretic delivery, which is no longer able to exercise control over the  
343 absorption of the drug when the stratum corneum has been compromised.

344 Finally, a summary of the passive and iontophoretic transport of phenobarbital  
345 as a function of TEWL (reflecting barriers of varying competence) is shown in Figure  
346 7. The slopes of the linear regressions through the passive and iontophoretic fluxes  
347 are not significantly different. This emphasizes the point made above that, once the  
348 function of the stratum corneum has been undermined (>50%), the passive transport



349 of phenobarbital exceeds that due to iontophoresis and dominates the transdermal  
350 delivery of the drug.

### 351 **3.4 Feasibility of phenobarbital transdermal delivery**

352 Phenobarbital is used for different purposes in neonatal and paediatric patients.  
353 Examination of the doses used for different indications (BNF for children 2011, Bio,  
354 2011; Finnegan, 2005; Osborn, 2010) quickly reveals that the transdermal route  
355 would not provide the initially large doses required to treat status epilepticus (20  
356  $\text{mg}\cdot\text{kg}^{-1}$  for neonates) or the loading doses required for epilepsy and neonatal  
357 abstinence syndrome. However, the maintenance doses for status epilepticus are  
358 much lower:  $2.5\text{-}5\text{ mg}\cdot\text{kg}^{-1}$  once or twice a day for both neonates and children aged 1  
359 month to 12 years (BNF for children 2011). For epilepsy, the maintenance doses are  
360  $2.5\text{-}5\text{ mg}\cdot\text{kg}^{-1}\cdot\text{day}^{-1}$  and up to  $2.5\text{-}8\text{ mg}\cdot\text{kg}^{-1}\cdot\text{day}^{-1}$  for neonates and children (1 month-  
361 12 years) respectively, (BNF for children 2011). The maintenance doses  
362 recommended for treating neonatal withdrawal symptoms fall in the range  $2\text{-}10$   
363  $\text{mg}\cdot\text{kg}^{-1}\cdot\text{day}^{-1}$  (Bio, 2011; Finnegan, 2005; Osborn, 2010). The phenobarbital doses  
364 required for any of the indications mentioned in children older than 12 years are too  
365 large for transdermal administration.

366 Table 3 calculates the passive and iontophoretic patch sizes required to deliver  
367 maintenance doses between  $2$  and  $10\text{ mg}\cdot\text{kg}^{-1}\cdot\text{day}^{-1}$  ( $0.3$  to  $1.6\text{ }\mu\text{mol}\cdot\text{kg}^{-1}\cdot\text{h}^{-1}$ ) i.e.,  
368 amounts spanning the three potential applications of phenobarbital discussed  
369 above. The fluxes used in these calculations were those measured when the donor  
370 solution was  $50\text{ mM}$  of drug in water at  $\text{pH } 8.5$ .

371 Assuming a quantitative *in vitro-in vivo* correlation, transdermal delivery of  
372 phenobarbital to neonates (including premature and full-term) appears feasible.

373 Indeed, passive would be sufficient for premature neonates with significantly  
374 immature skin. However, as the skin barrier matures, iontophoresis would become  
375 progressively more effective in providing desirable rates of delivery while keeping  
376 patch size reasonable (Table 3). For safety reasons, and the variable degree of barrier  
377 immaturity in the premature neonate, transdermal patches with rate-limiting  
378 membranes may be preferable, to ensure rate-control and to avoid potential  
379 toxicity. A key challenge with premature neonates is to compensate the rate of drug  
380 delivery for the degree of barrier maturation.

381 Premature neonates of only 23-25 weeks gestational age may require more  
382 than 4 weeks to develop a full functional stratum corneum (Kalia, 1998); whereas  
383 those born at 32 weeks or more have a barrier function that is close to fully  
384 functional. To treat this “moving target” would require passive patches in a variety of  
385 sizes (and even designs, e.g., rate-controlling versus matrix); alternatively  
386 iontophoresis might prove more useful in that the intensity and duration of current  
387 can be “tuned” to provide the required drug input. This flexibility in dosage form  
388 design and operation would rely, of course, on the application of TEWL  
389 measurements to pinpoint barrier function status in the patient (Fluhr, 2006, Levin,  
390 2005).

391 Table 3 also shows that iontophoresis may deliver therapeutic amounts of  
392 phenobarbital to infants of 1 month or more to young children. For older children,  
393 however, phenobarbital transdermal delivery may not be useful because the  
394 requisite patch area becomes too large. For example, the patch sizes required to  
395 deliver  $2-10 \text{ mg}\cdot\text{kg}^{-1}\cdot\text{day}^{-1}$  would be  $4-20 \text{ cm}^2$ ,  $6-32 \text{ cm}^2$ , and  $12-64 \text{ cm}^2$  for paediatric  
396 patients weighing 3, 5 and a 10 kg, respectively.

397           Ultimately, *in vivo* studies will be required to demonstrate that the *in vitro-in*  
398 *vivo* correlation assumed is valid and to examine the effect of current application  
399 and other formulation variables (such as pH) on the skin of infants and premature  
400 neonates.

#### 401           **4. Conclusions**

402           This study demonstrated that cathodal iontophoresis of phenobarbital through  
403 intact skin is more efficient than anodal iontophoresis and passive diffusion.  
404 Competition from anions present in the donor formulation must be minimized to  
405 optimize phenobarbital delivery. The results suggest that both passive and  
406 iontophoretic delivery of this drug to premature neonatal and paediatric patients  
407 may, in some circumstances, be feasible and attractive. Of course, the costs  
408 associated with the development and use of such new transdermal systems must be  
409 carefully balanced against their potential to provide an improved and better-  
410 tolerated therapy.

411

#### 412           **Acknowledgments**

413           A. Djabri is grateful to the Algerian Government for sponsoring her PhD.

414

415        **References**

416        Allagaert, K. et al., 2010. Prospective assessment of short-term propylene glycol  
417 tolerance in neonates. Arch. Dis. Child. 95, 1054-1058.

418        Bio, L. L. et al., 2011. Update on the pharmacological management of neonatal  
419 abstinence syndrome. J. Perinatol. 31, 692-701.

420        Blume et al., 2009. Neonatal seizures: treatment and treatment variability in 31  
421 United States pediatric hospitals. J. Child. Neurol. 24, 148-154.

422        BNF for children, 2010-2011. BMJ group, Pharmaceutical Press, and RCPCH  
423 Publications Ltd. London.

424        Bonina, F.P., et al., 1993. In-vitro percutaneous-absorption evaluation of  
425 phenobarbital through hairless mouse, adult and premature human skin. Int. J.  
426 Pharm. 98, 93-99.

427        Botha, J.H. et al., 1995. Determination of phenobarbitone population clearance  
428 values for south african children. Eur. J. Clin. Pharmacol. 48, 381-383.

429        Cober, M.P., Johnson, C.E. 2007. Stability of an extemporaneously prepared  
430 alcohol-free phenobarbital suspension. Am. J. Health-Syst. Pharm. 64, 644-646.

431        Colquhoun-Flannery, W., Wheeler, R. 1992. Treating neonatal jaundice with  
432 phenobarbitone: the inadvertent administration of significant doses of ethyl-alcohol.  
433 Arch. Dis. Child. 67, 152-152.

434        Escobar-Chavez, J.J., et al., 2008. The tape-stripping technique as a method for  
435 drug quantification in skin. J. Pharm. Pharm. Sci. 11, 104-130.

436 Fang, J.Y., et al., 2004. Transdermal iontophoresis of 5-fluorouracil combined  
437 with electroporation and laser treatment. *Int. J. Pharm.* 270, 241-249.

438 Farahmand, L. et al., 2009. Measuring transepidermal water loss: a comparative  
439 in vivo study of condenser-chamber, unventilated-chamber and open-chamber  
440 systems. *Skin Res. Tech.* 15, 392-398.

441 Finnegan, L. Kandall, S.R. 2005, Neonatal abstinence syndromes, in: Yaffe, S.J.,  
442 Aranda, J.V. (Eds), *Neonatal and pediatric pharmacology: therapeutic principles in*  
443 *practice*, third ed., Lippincott Williams & Wilkins, Philadelphia; London, pp. 848-860.

444 Fluhr, J.W., et al., 2006. Transepidermal water loss reflects permeability barrier  
445 status: validation in human and rodent in vivo and ex vivo models. *Exp. Dermatol.* 15,  
446 483-492.

447 Green, P., et al., 1992. In vitro and in vivo iontophoresis of a tripeptide across  
448 nude rat skin. *J. Control. Release.* 20, 209-217.

449 Harpin, V., Rutter, N., 1982. Percutaneous alcohol absorption and skin necrosis  
450 in a preterm infant. *Arch. Dis. Child.* 57, 477-479.

451 Heimann, G., Gladtko, E., 1977. Pharmacokinetics of phenobarbital in childhood.  
452 *Europ. J. Clin. Pharmacol.* 12, 305-310.

453 Kalia, Y.N., Nonato, L.B., Hund C.H., Guy, R.H., 1998. Development of skin  
454 barrier function in premature infants. *J. Invest. Dermatol.* 111, 320-326.

455 Imhof, R.E., et al., 2009. Closed-chamber transepidermal water loss  
456 measurement: microclimate, calibration and performance. *Int. J. Cosmet. Sci.*, 31,  
457 97-118.

458 Leboulanger, B., et al. 2004. Non-invasive monitoring of phenytoin by reverse  
459 iontophoresis. *Eur. J. Pharm. Sci.*, 22, 427-433.

460 Lehr, V.T. et al., 2005. Anticonvulsants, in: Yaffe, S.J., Aranda, J.V. (Eds),  
461 Neonatal and pediatric pharmacology: therapeutic principles in practice, third ed.,  
462 Lippincott Williams & Wilkins, Philadelphia; London, pp. 504-519.

463 Levin, J., and Maibach H. 2005. The correlation between transepidermal water  
464 loss and percutaneous absorption: An overview. *J. Control. Release*, 103, 291-299.

465 The Merck Index, 2006. 14<sup>th</sup> Ed. Merck & Co. Inc. Whitehouse Station, NJ, USA.

466 Merino, V., et al., 1999. Electrorepulsion versus electroosmosis: effect of pH on  
467 the iontophoretic flux of 5-fluorouracil. *Pharm. Res.* 16, 758-761.

468 Mudry, B., et al., 2006. Prediction of iontophoretic transport across the skin. *J.*  
469 *Control. Release.* 111, 362-367.

470 Osborn D.A. et al., 2010. Sedatives for opiate withdrawal in newborn infants.  
471 *The Cochrane Library*, 10, 1-44.

472 Ouvrier, R.A., Goldsmith, R., Hey, E., 1982. Phenobarbitone dosage in neonatal  
473 convulsions. *Arch. Dis. Child.* 57, 653-657.

474 Phipps, J.B. and Gyory, J.R. 1992. Transdermal ion migration. *Adv. Drug. Deliv.*  
475 *Rev. 9*, 137-176.

476 Rubio et al., 2011. Barrier function of intact and impaired skin: percutaneous  
477 penetration of caffeine and salicylic acid. *Int. J. Dermatol.* 50, 881-889.

478 Sekkat, N., Kalia, Y.N., Guy, R.H., 2004a. Development of an in vitro model for  
479 premature neonatal skin: biophysical characterization using transepidermal water  
480 loss. *J. Pharm. Sci.* 93, 2936-2940.

481 Sekkat, N., Kalia, Y.N., Guy, R.H., 2004b. Porcine ear skin as a model for the  
482 assessment of transdermal drug delivery to premature neonates. *Pharm. Res.* 21,  
483 1390-1397.

484 Sylvestre, J.P., et al., 2008a. Iontophoresis of dexamethasone phosphate:  
485 competition with chloride ions. *J. Control. Release*, 131, 41-46.

486 Sylvestre, J.P., et al., 2008b. In vitro optimization of dexamethasone phosphate  
487 delivery by iontophoresis. *Phys. Ther.*, 88, 1177-1187.

488 Touw, D.J., et al., 2000. Clinical pharmacokinetics of phenobarbital in neonates.  
489 *Eur. J. Pharm. Sci.* 12, 111-116.

490 Winter M.E., 2010. *Basic clinical pharmacokinetics*, fifth ed. Lippincott William &  
491 Wilkins, Philadelphia.

492

493

494 **Table 1:** Experiments performed to characterise phenobarbital transdermal

495 delivery through intact, pretreated and impaired skin.

Skin barrier	Donor	PHEN (mM)	Experiment settings and duration	n	
Intact	Water (pH 8.5)	50	(1) Cathodal iontophoresis (5h), then passive diffusion (5h)	3	
			Passive diffusion (24h)	3	
	50 mM NaCl (pH 7.4)	15	(2) Cathodal iontophoresis (5h)	4	
			Anodal iontophoresis (5h)	4	
			Passive diffusion (24h)	6	
	Water (pH 7.4)	15	(3) Cathodal iontophoresis (5h)	6	
			(4) Cathodal iontophoresis (5h). Donor solution exchanged hourly	5	
	10 mM HEPES (pH 7.4)	15	(5) Cathodal iontophoresis (5h). Donor solution exchanged hourly	5	
	Pre-treated	Water (pH 8.5)	50	Pre-treatment: 0.4 mA for 5 h followed by passive diffusion (24h)	4
	Impaired: 20-40 % 60-80 % 100 %	Water (pH 8.5)	50	Cathodal iontophoresis (5h), then passive diffusion (5h)	3-5
Passive diffusion (24h)				3-5	

496

497



498 **Table 2:** Fluxes of phenobarbital ( $\mu\text{mol}\cdot\text{h}^{-1}$ , mean  $\pm$  SD), through differentially-  
 499 impaired skin barriers, after 5 hours of iontophoresis, and after a further 5 hours of  
 500 passive diffusion post-current application. The corrected values ( $J_{\text{COR,PHEN}}$ ) are the  
 501 differences between the measurements in the first two columns and are used to  
 502 calculate the transport number ( $t_{\text{PHEN}}$ ) shown.

503

Skin barrier	Iontophoresis $J_{\text{PHEN}}$	Passive post- iontophoresis	Corrected $J_{\text{COR,PHEN}}$	$10^2 \times t_{\text{PHEN}}$
Intact	$0.34 \pm 0.06$	$0.05 \pm 0.01$	$0.30 \pm 0.07$	$2.0 \pm 0.4$
Intermediate "less"	$0.60 \pm 0.09$	$0.24 \pm 0.08$	$0.35 \pm 0.08$	$2.4 \pm 0.5$
Intermediate "plus"	$0.94 \pm 0.27$	$0.63 \pm 0.31$	$0.31 \pm 0.09$	$2.1 \pm 0.6$
Fully compromised	$1.23 \pm 0.32$	$0.92 \pm 0.25$	$0.31 \pm 0.08$	$2.1 \pm 0.5$

504

505

506

507

508

509 **Table 3:** Estimated patch sizes required to deliver maintenance doses of  
 510 phenobarbital assuming that the *in vitro* fluxes determined in this work are reflective  
 511 of those achievable *in vivo*.

512

Skin type:	Intact	Intermediate "less"	Intermediate "plus"	Fully compromised
<i>Passive</i>				
<i>In vitro</i> flux ( $\mu\text{mol}\cdot\text{h}^{-1}\cdot\text{cm}^{-2}$ ) <sup>a</sup>	<i>Negligible</i>	$0.1 \pm 0.02$	$0.8 \pm 0.2$	$1.1 \pm 0.4$
Patch size required ( $\text{cm}^2\cdot\text{kg}^{-1}$ )		3 – 16	0.4 – 2	0.3 – 1.5
<i>Iontophoresis (0.5 mA.cm<sup>-2</sup>)</i>				
<i>In vitro</i> flux ( $\mu\text{mol}\cdot\text{h}^{-1}\cdot\text{cm}^{-2}$ ) <sup>a</sup>	$0.5 \pm 0.1$	$0.7 \pm 0.1$	$1.2 \pm 0.4$	$1.5 \pm 0.4$
Area per electrode ( $\text{cm}^2\cdot\text{kg}^{-1}$ )	0.6 – 3.2	0.4 – 2.3	0.25 – 1.3	0.2 – 1.1
Total patch size ( $\text{cm}^2\cdot\text{kg}^{-1}$ ) <sup>b</sup>	1.2 – 6.4	0.8 – 4.6	0.5 – 2.6	0.4 – 2.2

513

514 <sup>a</sup> Fluxes are the average values measured after 2 – 5 hours of iontophoresis ( $0.5 \text{ mA}\cdot\text{cm}^{-2}$ ) or  
 515 passive diffusion.

516 <sup>b</sup> Assuming that the areas occupied by the anodal and cathodal electrode formulations are  
 517 the same.

518

519

520

521

### Figure legends

522

523 **Figure 1:** Passive diffusion of phenobarbital through intact pig skin. Pre-  
524 treatment either involved 5 hours direct current at 0.4 mA or 5 hours hydration  
525 without current. Phenobarbital was not present in the pre-treatment periods. Data  
526 are represented as the mean  $\pm$  SD.

527

528

529 **Figure 2:** Passive and iontophoretic transdermal fluxes (mean  $\pm$  SD) of  
530 phenobarbital after 5 hours from a 50 mM drug solution.

531

532

533 **Figure 3:** Anodal and cathodal iontophoresis of phenobarbital when delivered  
534 from a 15 mM drug solution at pH 7.4. The passive diffusion control is also shown.  
535 Data points are represented as mean  $\pm$  SD.

536

537

538 **Figure 4:** *Left panel:* Estimated donor concentration of chloride ions (dashed  
539 lines) and the corresponding measurements (symbols, mean  $\pm$  SD) for experiments 3  
540 ( $\blacktriangle$ ), 4 ( $\square$ ), and 5 ( $\bullet$ ) as indicated in Table 1. *Right panel:* Cathodal delivery of  
541 phenobarbital from different donor solutions (pH 7.4) containing various amounts of  
542 competing co-ions (experiments 2-5 in Table 1). The flux values (mean  $\pm$  SD) were  
543 determined after 5 hours of iontophoresis (0.4 mA).

544 **Figure 5:** Transport number of phenobarbital ( $t_{\text{PHEN}}$ , mean  $\pm$  SD) as a function of  
545 molar fraction ( $X_{\text{PHEN}}$ ). Values of the latter parameter were calculated from the  
546 concentrations of phenobarbital, HEPES, and chloride. The sources of  $\text{Cl}^-$  included  
547 NaCl (used as background electrolyte), HCl (used to adjust the donor solution pH),  
548 and the electrode electrochemical reaction. Data expressed by the same symbol and  
549 number represent the experimental condition as identified in Table 1. The dashed  
550 line is the linear regression through all data points except those obtained with  
551 HEPES:  $t_{\text{PHEN}} = 0.002 (\pm 0.001) + 0.033 (\pm 0.002) X_{\text{PHEN}}$ , ( $r^2 > 0.8$ ).

552  
553

554 **Figure 6:** Passive (left panel) and iontophoretic (right panel) transport (mean  $\pm$   
555 SD) of phenobarbital delivered from a 50 mM drug solution through intact and  
556 compromised skin barriers. The right panel also shows the passive diffusion of  
557 phenobarbital post-current termination at 5 hours.

558  
559

560 **Figure 7:** Total passive and iontophoretic fluxes of phenobarbital as a function  
561 of TEWL across skin barriers of different competencies. Open symbols refer to  
562 passive diffusion alone; filled symbols reflect the total drug flux when an  
563 iontophoretic current is applied. Intact, intermediate “less” (20–40 %), intermediate  
564 “plus” (60–80 %) and fully compromised skin barriers are respectively symbolized by  
565 diamonds, triangles, circles, and squares. Linear regressions through the passive and  
566 iontophoretic results were:  $J_{\text{Passive}} = -156 (\pm 97) + 8.3 (\pm 1.1) \cdot \text{TEW}$  and  $J_{\text{ionto}} = 372$   
567  $(\pm 101) + 7.0 (\pm 0.9) \cdot \text{TEWL}$ , with  $r^2$  values of 0.85 and 0.82, respectively.

Figure 1

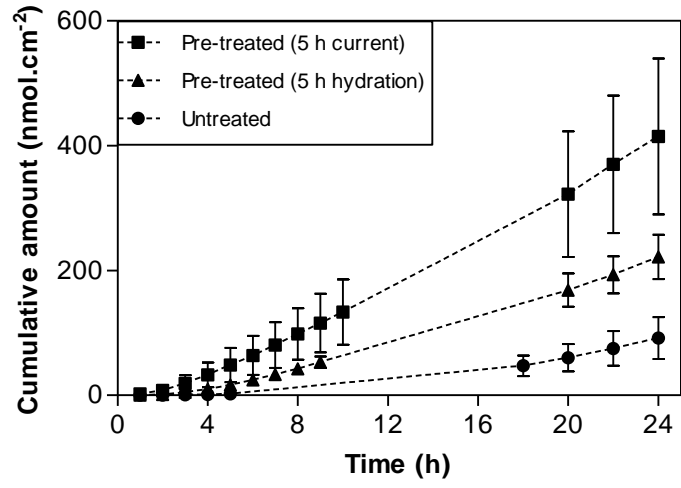


**Figure 2**

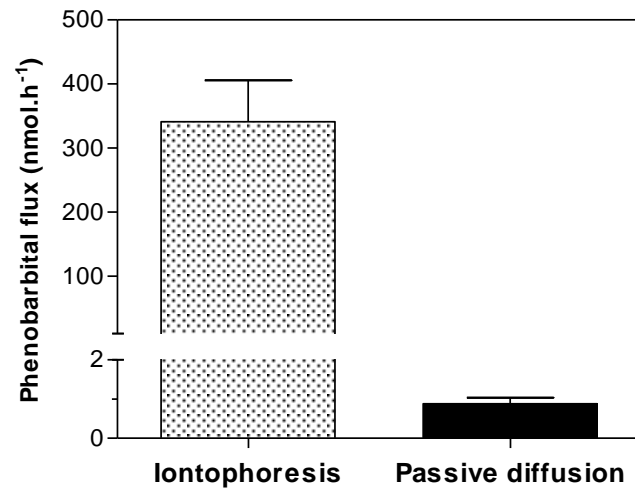


Figure 3

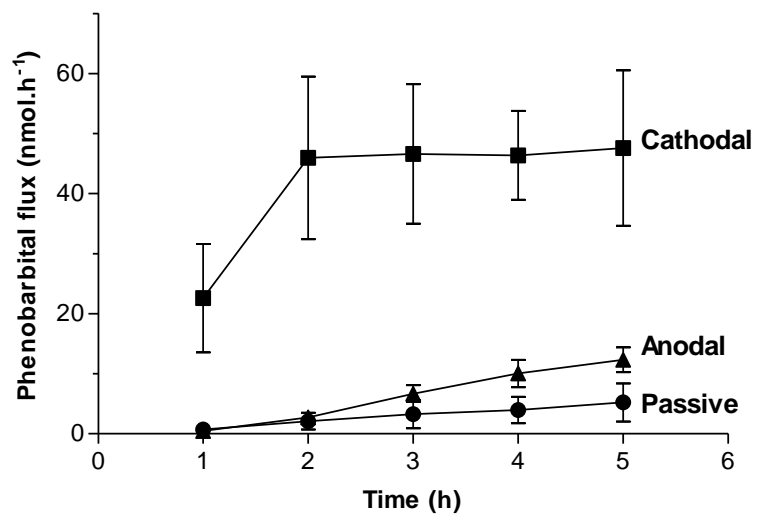


Figure 4

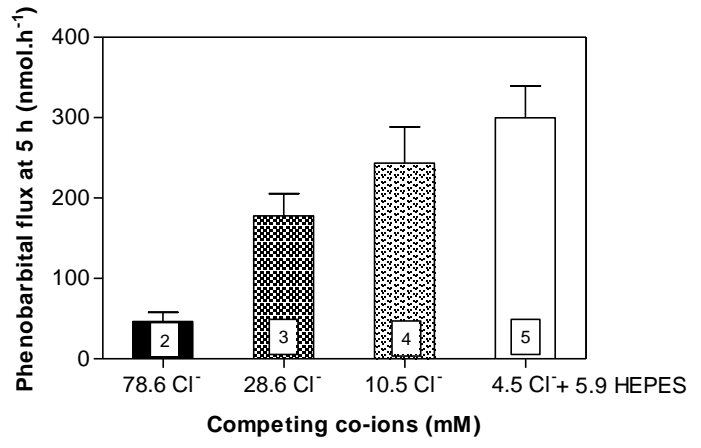
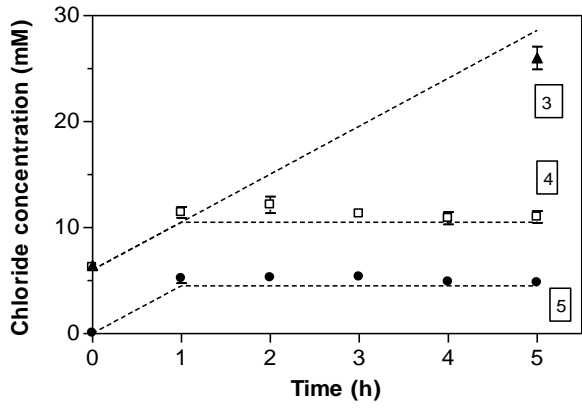




Figure 5

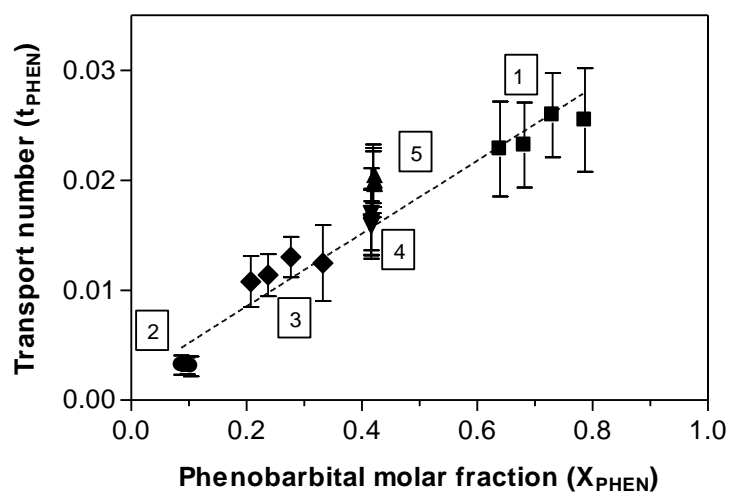


Figure 6

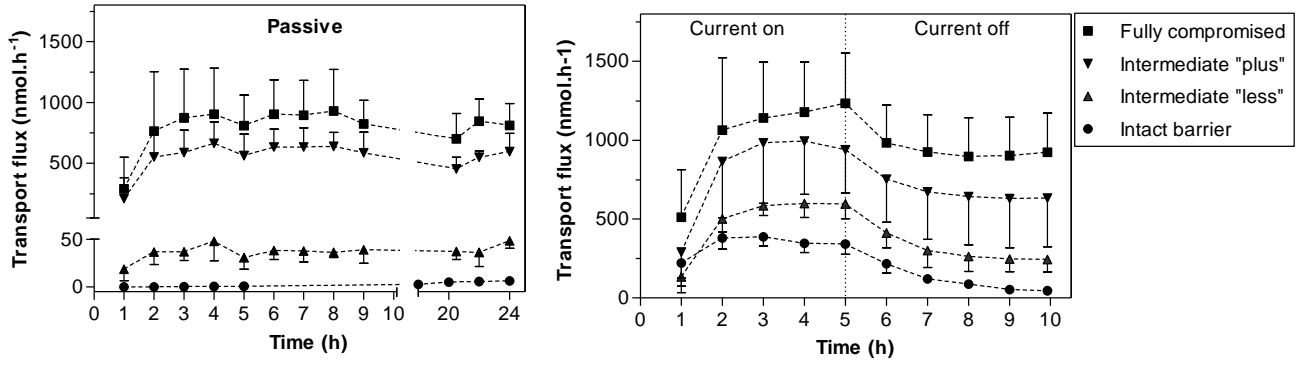


Figure 7

